Harmonics in the tunneling current for a nanocircuit with a mode-locked laser

Mark J. Hagmann, NewPath Research L.L.C.
2880 S. Main Street, Suite 214, Salt Lake City, Utah USA 84115

Abstract

Focusing a mode-locked laser on the tip-sample tunneling junction of a scanning tunneling microscope superimposes currents at hundreds of harmonics of the laser pulse-repetition rate on the DC tunneling current. The power at each harmonic is inversely proportional to the square of the frequency because of the measurement circuit. However, analysis suggests that within the tunneling junction the harmonics may have no appreciable roll-off at frequencies up to 45 THz. We consider a nanocircuit with an optical antenna receiving the laser radiation, metal-insulator-metal (MIM) tunneling diodes to generate the harmonics, and filters to select microwave and terahertz harmonics that are transmitted by a second antenna.

1. Background and introduction

Earlier, following simulations, we focused a mode-locked Ti:Sapphire laser on the tunneling junction of a scanning tunneling microscope (STM) to generate a unique microwave frequency comb (MFC) with hundreds of harmonics at integer multiples of the 74.25 MHz laser pulse-repetition frequency [1]. The 200^{th} harmonic, at 14.85 GHz, has a power of only 2.8 atto-watts but the signal-to-noise ratio is 25 dB. These extremely low-noise measurements are possible because the FWHM (full-width at half maximum) linewidth of each harmonic is only 1.2 Hz. Thus, the quality factor (Q) exceeds 10^{10} to set the present state-of-the-art for low-noise and low-power microwave measurements [2]. The measured linewidth is an upper bound as a convolution of the true linewidth with the response of the spectrum analyzer.

Figure 1 is a block diagram for the system we used to measure the harmonics with an STM. A section of 50-Ω coaxial cable connects the tip electrode of the STM to a spectrum analyzer. The impedance of the tunneling junction is much greater than the characteristic impedance of the cable so the cable acts as a capacitance of 6.4 pF across the 50-Ω input impedance of the spectrum analyzer. Thus, the current at each harmonic is divided between the resistive input of the spectrum analyzer and the capacitive shunt of the cable. This forms a low-pass filter, with a 3dB point of 500 MHz, which caused the power measured at the harmonics to roll-off as the inverse square of the frequency.

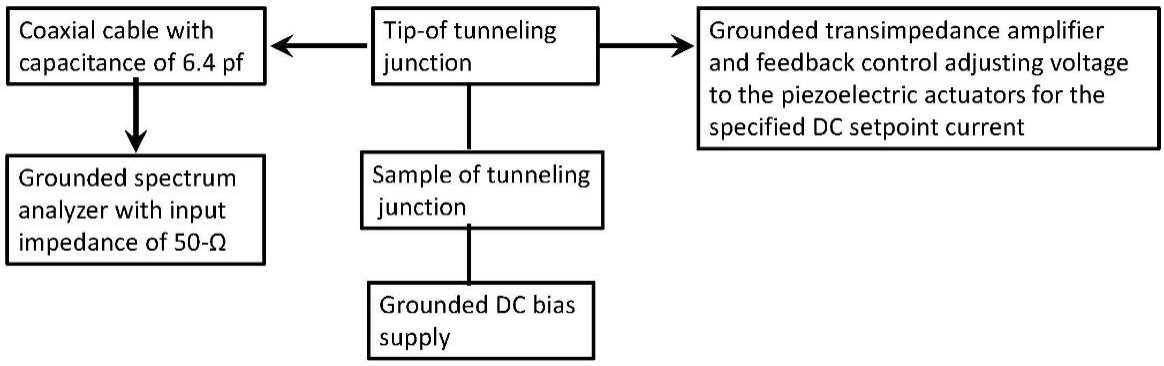

Fig. 1. Block diagram of the system used to measure the microwave harmonics with an STM.

Our simulations suggest that in laser-assisted quantum tunneling there is an inherent roll-off of the power ("cutoff") caused by quantum phenomena having a half-power point near 45 THz depending on the linewidth of the laser [3]. We are preparing to form a nanocircuit generating bands of adjacent harmonics at frequencies up to this cutoff. The extremely high accuracy and precision in our measurements of the microwave harmonics with an STM may enable extending this work to terahertz frequencies with the new nanocircuit that is described.

Outline of the presentation

Section 1 Background and Introduction
Section 2 Description of the new nanocircuit
Section 3 General expression for the current in each MIM tunneling diode
Section 4 Pattern of the electrical current within the nanocircuit
Section 5 Derivation for the current in a set of adjacent harmonics well below the cutoff
Section 6 Derivation of the current in a set of adjacent harmonics near the cutoff
Section 7 Derivation of the current in any set of adjacent harmonics
Section 8 Interference in summing the harmonics well below cutoff
Section 9 Limit for the current in a large set of adjacent harmonics
Section 10 Transmitting power at the harmonics with a thin-wire dipole antenna
Section 11 Solutions for examples
Section 12 Summary and conclusions

2. Description of the new nanocircuit

Now we consider the possibility of making a self-contained nanocircuit in which the roll-off in the measured power that is caused by the cabling to the tunneling junction in an STM is eliminated. Optical antennas are used to receive the radiation from a mode-locked laser and a dipole antenna transmits the harmonics in selected bands at microwave or terahertz frequencies (patent-pending).

Figure 2 is a sketch showing the design for the nanocircuit. Here "MIM" denotes two symmetrical metal-insulator-metal tunneling diodes that are used in place of the tunneling junction in the STM. The parasitic shunting capacitance of these diodes is not shown in this sketch but it is considerably less than the 6.4 pF capacitance that shunts the 50 Ω input impedance of the spectrum analyzer in our STM measurements. This sketch is not made to scale because the relative length of the vertical dipole will be much greater.

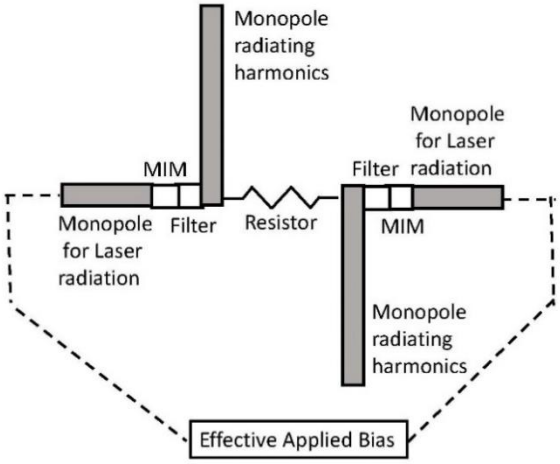

Fig. 2. Sketch of the nanocircuit generating and microwave and terahertz harmonics.

Instead of focusing a laser directly on the tunneling junction, as we did with the STM, here the laser interacts with the optical monopole antennas at the left and right ends of the sketch. This causes a voltage having the full laser spectrum across each MIM diode, which we label as the "effective applied bias", caused by the mode-locked laser. This voltage has opposite polarities at the left and right ends of the nanocircuit for the applied bias. However, the two filters prevent the spectrum of the laser from reaching the circuit that is between them. The current at the harmonics, which is generated in the two MIM diodes passes through the resistor at the center of the sketch. This resistor is at the feed-point for the dipole which is formed by the two vertical monopole antennas. Thus, the voltage drop across this resistor causes this dipole to radiate at the bands of microwave or terahertz harmonics which are chosen when designing the two filters. A resistive L-network could also be added at each end of this resistor to improve the impedance matching to the vertical antenna.

3. General expression for the current in each MIM tunneling diode

Previously [3] we showed that, if the load resistor R_L could be located within the tunneling junction, the power at the k-th harmonic would be given by Eq. (1) where P_1 is the power at the first harmonic. Thus, within the tunneling junction, Thus, Eq. (2) gives the current at the k-th harmonic where I_1 is the peak value of the current at the first harmonic where n is 1. Here "T" is the time between consecutive laser pulses and "τ" is the duration of each pulse. The quantity τ/T, which is the fraction of the time that a pulse is active, is very small with a mode-locked laser. In measurements with an STM [1], a power of -120 dBm was measured at the first harmonic with a spectrum analyzer having an input impedance of 50 Ω so I_1 would be 6 nA.

$$P_k = P_1 e^{-\pi^2 (k-1)^2 \left(\frac{\tau}{T}\right)^2} \tag{1}$$

$$I_k = I_1 \sin\left(k\omega_0 t\right) e^{-\frac{\pi^2 \tau^2}{2T^2}(k-1)^2} \tag{2}$$

Now we simplify Eq. (2) to give Eq. (3) where A is the positive parameter that is defined in Eq. (4) and k is a number much greater than 1.

$$I_k = I_1 \sin\left(k\omega_0 t\right) e^{-Ak^2} \tag{3}$$

$$A \equiv \frac{\pi^2}{2}\left(\frac{\tau}{T}\right)^2 \tag{4}$$

We refer to the phenomena that occur where Ak^2 is comparable to 1 as "cutoff" because the exponential decay in the current becomes prominent at frequencies above that point.

4. Pattern of the electrical current within the nanocircuit

Figure 3 shows the components of the current within the nanocircuit. The filtered current from the MIM diode splits into two components, one going through the resistor and the other going to the upper monopole. The current going through the resistor splits into two components, one going to the second MIM diode and the other through the lower monopole. Determining the current in the nanocircuit would require knowing the radiation resistance and reactance of each vertical monopole, the value of the resistor, and the spectrum of the filtered current from the MIM diode.

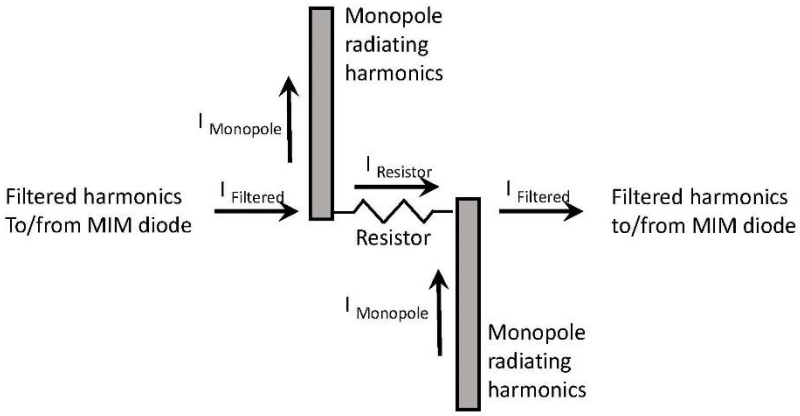

Fig. 3. Components of the current within the nanocircuit.

In any application of this technology a specific part of the spectrum would be selected by the filters. In order to provide an overview of some of the possibilities we consider the effect of having a set of consecutive harmonics of the fundamental angular frequency ω_0 for the pulse repetition rate of the laser as defined in Eq. (5). Thus, at time t the total current would be given by Eq. (6).

$$\omega_k \equiv k\omega_0, \text{ where the integer } k_1 \le k \le k_2 \tag{5}$$

$$I(t) = I_1 \sum_{k=k_1}^{k_2} \sin(k\omega_0 t) e^{-Ak^2} \tag{6}$$

Now, we solve the general expression in Eq. (6) to obtain closed-form algebraic expressions for the total current with sets of adjacent harmonics that are well below the cutoff frequency (Section 5) and near the cutoff frequency (Section 6), as well as for the more general case (Section 7). Sets of adjacent harmonics are of special interest because large numbers of harmonics may be within the usable passband of the transmitting antenna at terahertz frequencies to provide greater output power.

5. Derivation for the current in a set of adjacent harmonics well below the cutoff

As already noted, at the higher harmonics, the exponential in Eq. (6) causes a cutoff where the current decays to zero. However, first we make the approximation of setting the exponential to unity for solutions that correspond to frequencies well below the cutoff. We derived the identity shown as Eq. (7) using Wolfram Alpha, verified it, and used it with Eq. (6) to obtain Eq. (8) as a for the total current as a function of time with all of the harmonics in the interval $k_1 \le k \le k_2$. Numerical testing has verified that our calculations made by summing many terms using Eq. (6) to determine the current as a function of time agree with the closed-form for this summation in Eq. (8).

$$\sum_{k=k_1}^{k_2} \sin(kx) \equiv \frac{1}{2}\left[\begin{array}{l} \sin(k_1 x) + \cot\left(\frac{x}{2}\right)\cos(k_1 x) \\ +\sin(k_2 x) - \cot\left(\frac{x}{2}\right)\cos(k_2 x) \end{array}\right] \tag{7}$$

$$I(t)=\frac{I_1}{2}\left[\begin{array}{l}\sin\left(k_1\omega_0 t\right)+\cot\left(\frac{\omega_0 t}{2}\right)\cos\left(k_1\omega_0 t\right)\\+\sin\left(k_2\omega_0 t\right)-\cot\left(\frac{\omega_0 t}{2}\right)\cos\left(k_2\omega_0 t\right)\end{array}\right] \quad (8)$$

6. Derivation of the current in a set of adjacent harmonics near the cutoff

Let $\|I_k\|$ be the peak value for the magnitude of the current at the kth harmonic. Thus, because the spacing between adjacent harmonics is small near the cutoff, the value for the peak of the k+1 th harmonic is related to that for the k th harmonic by the following approximation:

$$\frac{\|I_{k+1}\|}{\|I_k\|}=\frac{e^{-A(k+1)^1}}{e^{-Ak^2}}=e^{-A(2k+1)} \quad (9)$$

For the Ti:Sapphire laser used in our measurements at Los Alamos the pulse duration τ is 6 fs. The pulse repetition rate is 74.25 MHz so the time between consecutive pulses, T is 13.5 ns. Thus, from Eq. 4, the parameter A is 9.7 x10^{-13}. In order to determine the value of k at which the peak power is one-half of that at the fundamental we label it as k_{3dB} to obtain Eq. (10), and write Eq. (11) for the current at the fundamental where k is 1.

$$\|I_{k_{3dB}}\|=I_1 e^{-Ak_{3dB}^2} \quad (10)$$

$$\|I_1\|=I_1 e^{-A} \quad (11)$$

Equation (12) is obtained by combining Eqs. (10) and (11). Thus, the ratio of the two values of power is given by Eq. (13). This ratio is defined to be one-half so we obtain Eq. (14) which is equivalent to Eq. (15). Rearranging Eq. (15) gives Eq. (16), and finally Eq. (17) as the value for the index k at the 3-dB point.

$$\frac{\|I_{k_{3dB}}\|}{\|I_1\|}=e^{A-Ak_{3dB}^2} \quad (12)$$

$$\frac{P_{k_{3dB}}}{P_1}=e^{2A-2Ak_{3dB}^2} \quad (13)$$

$$2e^{2A-2Ak_{3dB}^2}=1 \quad (14)$$

$$\ln(2)=2Ak_{3dB}^2-2A \quad (15)$$

$$\frac{\ln(2)}{2A}+1=k_{3dB}^2 \quad (16)$$

$$k_{3dB}=\sqrt{1+\frac{\ln(2)}{2A}} \quad (17)$$

We have already noted that in our measurements of the microwave frequency comb with an STM, A was approximately 9.7 x10^{-13}. Thus, Eq. (17) shows that k_{3dB} would be 6.0 x10^5 corresponding to a frequency of 45 THz. However, as already noted, this would only pertain if measurements were made within the tip-sample tunneling junction of the STM which has not been possible.

Next, consider a small band of harmonics with $k_1 \le k \le k_2$ where k_1 and k_2 are large. When the range of this band, defined as k_2 minus k_1, is much smaller than either k_1 or k_2 there will be little variation in the value of the exponential for the argument of the summation in Eq. (6). Thus,

we approximate Eq. (6) with Eq. (18) where $\bar{k}$ is the mean value for k_1 and k_2. The summation in Eq. (7) is used in Eq. (18) to obtain Eq. (19) as an approximation for the total current in the range from k_1 to k_2.

$$I(t) = I_1 e^{-A\bar{k}^2} \sum_{k=k_1}^{k=k_2} \sin(k\omega_0 t) \tag{18}$$

$$I(t) = \frac{I_1}{2} e^{-A\bar{k}^2} \left[\begin{array}{l} \sin(k_1\omega_0 t) + \cot\left(\frac{\omega_0 t}{2}\right)\cos(k_1\omega_0 t) \\ +\sin(k_2\omega_0 t) - \cot\left(\frac{\omega_0 t}{2}\right)\cos(k_2\omega_0 t) \end{array} \right] \tag{19}$$

Note that Eq. (19) is appropriate for calculating the current with clusters of harmonics near cutoff where there is a small range for the parameter k. However, we anticipate that the spectrum of the harmonics near cutoff would depend strongly on the stability of the mode-locked laser.

7. Derivation of the current in any set of adjacent harmonics

The Taylor series expansion for the exponential in Eq. (6) is given by Eq. (20)

$$e^{-Ak^2} = \sum_{n=0}^{\infty} \frac{\left(-Ak^2\right)^n}{n!} \tag{20}$$

Combining Eqs. (6) and (20) gives Eq. (21) for the total current where x is defined as $\omega_0 t$.

$$I(t) = I_1 \sum_{k=k_1}^{k=k_2} \left[\sin(kx) \sum_{n=0}^{\infty} \frac{\left(-Ak^2\right)^n}{n!} \right] \tag{21}$$

Writing the first few terms of the new summation in Eq. (21 gives Eq. (22) for the current.

$$I(t) = I_1 \sum_{k=k_1}^{k=k_2} \left[\sin(kx) \left\{ 1 - \frac{Ak^2}{1!} + \frac{A^2k^4}{2!} - \frac{A^3k^6}{3!} + \frac{A^4k^8}{4!} - \frac{A^5k^{10}}{5!} + \cdots \right\} \right] \tag{22}$$

Next, the terms of the explicit inner summation in Eq. (22) are separated. The first sum denoted by T_1 is Eq. (23), which was obtained earlier using Wolfram Alpha as Eq. (7). The sums corresponding to the other 5 terms in Eq. (22), which were also obtained using Wolfram Alpha, are used in Eqs. (24) through (28).

$$T_1 \equiv \sum_{k=k_1}^{k_2} \sin(kx) = \frac{1}{2}\left[\sin(k_1 x) + \cot\left(\frac{x}{2}\right)\cos(k_1 x) + \sin(k_2 x) - \cot\left(\frac{x}{2}\right)\cos(k_2 x) \right] \tag{23}$$

$$T_2 = -\frac{A}{1!} \sum_{k=k_1}^{k=k_2} k^2 \sin(kx) = -\frac{A}{1} x^2 \csc\left(\frac{x}{2}\right) \sin\left[\frac{1}{2}(1 - k_1 + k_2)x\right] \sin\left[\frac{1}{2}(n_1 + n_2)x\right] \tag{24}$$

$$T_3 = \frac{A^2}{2!} \sum_{k=k_1}^{k=k_2} k^4 \sin(kx) = \frac{A^2}{2!} x^4 \csc\left(\frac{x}{2}\right) \sin\left[\frac{1}{2}(1 - k_1 + k_2)x\right] \sin\left[\frac{1}{2}(k_1 + k_2)x\right] \tag{25}$$

$$T_4 = -\frac{A^3}{3!} \sum_{k=k_1}^{k=k_2} k^6 \sin(kx) = -\frac{A^3}{3!} x^6 \csc\left(\frac{x}{2}\right) \sin\left[\frac{1}{2}(1 - k_1 + k_2)x\right] \sin\left[\frac{1}{2}(k_1 + k_2)x\right] \tag{26}$$

$$T_5 = \frac{A^4}{4!} \sum_{k=k_1}^{k=k_2} k^8 \sin(kx) = \frac{A^4}{4!} x^8 \csc\left(\frac{x}{2}\right) \sin\left[\frac{1}{2}(1 - k_1 + k_2)x\right] \sin\left[\frac{1}{2}(k_1 + k_2)x\right] \tag{27}$$

$$T_6 = -\frac{A^5}{5!}\sum_{k=k_1}^{k=k_2} k^{10}\sin(kx) = -\frac{A^5}{5!}x^{10}\csc\left(\frac{x}{2}\right)\sin\left[\frac{1}{2}(1-k_1+k_2)x\right]\sin\left[\frac{1}{2}(k_1+k_2)x\right] \quad (28)$$

Setting x equal to $\omega_0 t$ and simplifying Eqs. (23) to (28) gives Eqs. (29) through (34).

$$T_1 = \frac{1}{2}\left[\sin(k_1\omega_0 t) + \cot\left(\frac{\omega_0 t}{2}\right)\cos(k_1\omega_0 t) + \sin(k_2\omega_0 t) - \cot\left(\frac{\omega_0 t}{2}\right)\cos(k_2\omega_0 t)\right] \quad (29)$$

$$T_2 = -\frac{A}{1}(\omega_0 t)^2\csc\left(\frac{\omega_0 t}{2}\right)\sin\left[\frac{1}{2}(1-k_1+k_2)\omega_0 t\right]\sin\left[\frac{1}{2}(k_1+k_2)\omega_0 t\right] \quad (30)$$

$$T_3 = \frac{A^2}{2!}(\omega_0 t)^4\csc\left(\frac{\omega_0 t}{2}\right)\sin\left[\frac{1}{2}(1-k_1+k_2)\omega_0 t\right]\sin\left[\frac{1}{2}(k_1+k_2)\omega_0 t\right] \quad (31)$$

$$T_4 = -\frac{A^3}{3!}(\omega_0 t)^6\csc\left(\frac{\omega_0 t}{2}\right)\sin\left[\frac{1}{2}(1-k_1+k_2)\omega_0 t\right]\sin\left[\frac{1}{2}(k_1+k_2)\omega_0 t\right] \quad (32)$$

$$T_5 = \frac{A^4}{4!}(\omega_0 t)^8\csc\left(\frac{\omega_0 t}{2}\right)\sin\left[\frac{1}{2}(1-k_1+k_2)\omega_0 t\right]\sin\left[\frac{1}{2}(k_1+k_2)\omega_0 t\right] \quad (33)$$

$$T_6 = -\frac{A^5}{5!}(\omega_0 t)^{10}\csc\left(\frac{\omega_0 t}{2}\right)\sin\left[\frac{1}{2}(1-k_1+k_2)\omega_0 t\right]\sin\left[\frac{1}{2}(k_1+k_2)\omega_0 t\right] \quad (34)$$

Thus, the total current is given as a function of time by multiplying I_1 by the sum of the RHS in Eqs. (29) through (34) to obtain Eq. (35), which is factored to obtain Eq. (36).

$$\begin{aligned} I(t) = {} & \frac{I_1}{2}\left[\sin(k_1\omega_0 t) + \cot\left(\frac{\omega_0 t}{2}\right)\cos(k_1\omega_0 t) + \sin(k_2\omega_0 t) - \cot\left(\frac{\omega_0 t}{2}\right)\cos(k_2\omega_0 t)\right] \\ & - \frac{AI_1}{1!}(\omega_0 t)^2\csc\left(\frac{\omega_0 t}{2}\right)\sin\left[\frac{1}{2}(1-k_1+k_2)\omega_0 t\right]\sin\left[\frac{1}{2}(k_1+k_2)\omega_0 t\right] \\ & + \frac{A^2 I_1}{2!}(\omega_0 t)^4\csc\left(\frac{\omega_0 t}{2}\right)\sin\left[\frac{1}{2}(1-k_1+k_2)\omega_0 t\right]\sin\left[\frac{1}{2}(k_1+k_2)\omega_0 t\right] \\ & - \frac{A^3 I_1}{3!}(\omega_0 t)^6\csc\left(\frac{\omega_0 t}{2}\right)\sin\left[\frac{1}{2}(1-k_1+k_2)\omega_0 t\right]\sin\left[\frac{1}{2}(k_1+k_2)\omega_0 t\right] \\ & + \frac{A^4 I_1}{4!}(\omega_0 t)^8\csc\left(\frac{\omega_0 t}{2}\right)\sin\left[\frac{1}{2}(1-k_1+k_2)\omega_0 t\right]\sin\left[\frac{1}{2}(k_1+k_2)\omega_0 t\right] \\ & - \frac{A^5 I_1}{5!}(\omega_0 t)^{10}\csc\left(\frac{\omega_0 t}{2}\right)\sin\left[\frac{1}{2}(1-k_1+k_2)\omega_0 t\right]\sin\left[\frac{1}{2}(k_1+k_2)\omega_0 t\right] + \cdots \end{aligned} \quad (35)$$

$$\begin{aligned} I(t) = {} & \frac{I_1}{2}\left[\sin(k_1\omega_0 t) + \cot\left(\frac{\omega_0 t}{2}\right)\cos(k_1\omega_0 t) + \sin(k_2\omega_0 t) - \cot\left(\frac{\omega_0 t}{2}\right)\cos(k_2\omega_0 t)\right] \\ & - I_1\left[\frac{A}{1!}(\omega_0 t)^2 - \frac{A^2}{2!}(\omega_0 t)^4 + \frac{A^3}{3!}(\omega_0 t)^6 - \frac{A^4}{4!}(\omega_0 t)^8 + \frac{A^5}{5!}(\omega_0 t)^{10} - \cdots\right] \\ & \csc\left(\frac{\omega_0 t}{2}\right)\sin\left[\frac{1}{2}(1-k_1+k_2)\omega_0 t\right]\sin\left[\frac{1}{2}(k_1+k_2)\omega_0 t\right] \end{aligned} \quad (36)$$

We use the Taylor series in Eq. (37), that is modified in Eq. (38) and used to change the summation on the second line of Eq. (36) so that the second line of Eq. (35) may be written as Eq. (40).

$$e^{-x} = 1 - \frac{x}{1!} + \frac{x^2}{2!} - \frac{x^3}{3!} + \frac{x^4}{4!} - \frac{x^5}{5!} + \cdots \tag{37}$$

$$1 - e^{-x} = \frac{x}{1!} - \frac{x^2}{2!} + \frac{x^3}{3!} - \frac{x^4}{4!} + \frac{x^5}{5!} + \cdots \tag{38}$$

$$1 - e^{-A(\omega_0 t)^2} \equiv \frac{A(\omega_0 t)^2}{1!} - \frac{A^2(\omega_0 t)^4}{2!} + \frac{A^3(\omega_0 t)^6}{3!} - \frac{A^4(\omega_0 t)^8}{4!} + \frac{A^5(\omega_0 t)^{10}}{5!} - \cdots \tag{39}$$

$$I(t) = \frac{I_1}{2}\left[\sin(k_1\omega_0 t) + \cot\left(\frac{\omega_0 t}{2}\right)\cos(k_1\omega_0 t) + \sin(k_2\omega_0 t) - \cot\left(\frac{\omega_0 t}{2}\right)\cos(k_2\omega_0 t)\right]$$
$$- I_1\left[1 - e^{-A(\omega_0 t)^2}\right]\csc\left(\frac{\omega_0 t}{2}\right)\sin\left[\frac{1}{2}(1 - k_1 + k_2)\omega_0 t\right]\sin\left[\frac{1}{2}(k_1 + k_2)\omega_0 t\right] \tag{40}$$

Equation (40) gives the total current as a function of time for a set of adjacent harmonics in the interval for $k_1 \le k \le k_2$. Well below cutoff, the second term of Eq. (40) is not significant so that Eq. (40) reduces to Eq. (8) which is periodic in interval for $\omega_0 t$ from 0 to 2π. However, near cutoff the second line of Eq. (40) must be included. Then, even with an ideal mode-locked laser, the current would not be periodic.

8. Interference in a set of adjacent harmonics well below cutoff

An ideal mode-locked laser would act as a "clock" so the full cycle for each harmonic of the current in the period $0 \le \omega_0 t \le 2\pi$, as well as the total current in any set of harmonics, would repeat to infinity. This may be understood from Eq. (8) in which the frequency at each harmonic of the current is an integer, or a half-integer, multiple of $\omega_0 t$ where ω_0 is 2π times the pulse-repetition frequency of the laser.

However, there are two cases where periodicity cannot take place. Firstly, the exponential in Eq. (40) shows that coherence is lost for harmonics near the cutoff. Secondly, the actual output of a mode-locked laser is a sequence of bursts of pulses, each burst having a similar length which is called the "coherence length". In deriving Eqs. (8) and (40) for the current, the ideal case was assumed for a laser having an infinite coherence length. The effects of having a finite coherence length must be considered later.

If a laser has a finite coherence length the process would restart at the end of each burst of pulses which would cause the output power from the harmonics to increase. There is an interesting paradox because shortening the coherence length of a mode-locked laser may actually increase the output power at the harmonics.

To model the operation of a mode-locked laser the current at each harmonic is zero at the start of each laser pulse. For the ideal case where the laser has an infinite coherence length, and operates well below the cutoff the total current is a decaying sinusoid with successive minima and maxima that are repeated in each consecutive laser pulse.

Regrouping the terms in Eq. (8) gives Eq. (41). Then, using the trigonometric identities in Eqs. (42) and (43), we obtain Eq. (44). Finally, simplifying Eq. (44) gives Eq. (45).

$$I(t) = \frac{I_1}{2}\left[\begin{array}{l}\sin(k_1\omega_0 t) + \sin(k_2\omega_0 t) \\ + \cot\left(\frac{\omega_0 t}{2}\right)\left[\cos(k_1\omega_0 t) - \cos(k_2\omega_0 t)\right]\end{array}\right] \tag{41}$$

$$\sin(\alpha)+\sin(\beta)\equiv 2\sin\left[\frac{\alpha+\beta}{2}\right]\cos\left[\frac{\alpha-\beta}{2}\right] \tag{42}$$

$$\cos(\alpha)-\cos(\beta)\equiv -2\sin\left[\frac{\alpha+\beta}{2}\right]\sin\left[\frac{\alpha-\beta}{2}\right] \tag{43}$$

$$I(t)=\frac{I_1}{2}\left[\begin{array}{l} 2\sin\left[\frac{(k_2+k_1)\omega_0 t}{2}\right]\cos\left[\frac{(k_2-k_1)\omega_0 t}{2}\right] \\ +2\sin\left[\frac{(k_2+k_1)\omega_0 t}{2}\right]\sin\left[\frac{(k_2-k_1)\omega_0 t}{2}\right]\cot\left(\frac{\omega_0 t}{2}\right)\end{array}\right] \tag{44}$$

$$I(t)=I_1\sin\left[(k_2+k_1)\frac{\omega_0 t}{2}\right]\left[\begin{array}{l}\cos\left[(k_2-k_1)\frac{\omega_0 t}{2}\right] \\ +\sin\left[(k_2-k_1)\frac{\omega_0 t}{2}\right]\cot\left(\frac{\omega_0 t}{2}\right)\end{array}\right] \tag{45}$$

The first term in Eq. (45) shows that the total current is zero at the times given by Eq. (46) where n is an integer and τ is the reciprocal of the laser pulse-repetition rate. Note that these nulls occur at closer intervals as k_1 and/or the number of harmonics is increased.

$$t_n=\frac{n\tau}{(k_1+k_2)} \tag{46}$$

Next, we consider a second case where the term within the brackets in Eq. (45) is zero as shown in Eq. (47).

$$\cos\left[(k_2-k_1)\frac{\omega_0 t}{2}\right]+\sin\left[(k_2-k_1)\frac{\omega_0 t}{2}\right]\cot\left(\frac{\omega_0 t}{2}\right)=0 \tag{47}$$

Simplifying Eq. (47) by setting k_2 equal to k_1 plus n, where n is a positive integer, gives Eq. (48).

$$\cos\left(\frac{n\omega_0 t}{2}\right)+\sin\left(\frac{n\omega_0 t}{2}\right)\cot\left(\frac{\omega_0 t}{2}\right)=0 \tag{48}$$

If $n\omega_0 t$ is an integer multiplied by 2π then the sine of $n\omega_0 t/2$ is zero. Otherwise, we may divide Eq. (48) by that sine term to obtain Eq. (49).

$$\cot\left(\frac{n\omega_0 t}{2}\right)=-\cot\left(\frac{\omega_0 t}{2}\right) \tag{49}$$

Using Eq. (49) where x is defined in Eq. (50) gives Eq. (51) where we are may choose any value for the integer n such that multiplying an arbitrary argument of the cotangent changes the sign of that function. However, for an arbitrary value of x, the actual value for n is generally not an integer. It is only possible to determine values of n that are integers for specific values of x.

$$x\equiv\frac{\omega_0 t}{2} \tag{50}$$

$$\cot(nx)=-\cot(x) \tag{51}$$

Thus, we have only the criterion in Eq. (46) to provide the most general solution for the sequence of times in which the total current is exactly zero which is caused by interference of the harmonics.

9. Limit for the current in a large set of adjacent harmonics

In the time-domain there is no current at time t equal to zero. This is followed by one dominant positive peak and subsequent positive and negative peaks having a monotonic decrease in their amplitude. As the total number of harmonics is increased the height of the first peak is increased and the rate of decay for the subsequent peaks becomes more pronounced. The total number of harmonics, which is given by $k_2 - k_1 + 1$, determines this behavior whether this is at gigahertz or terahertz frequencies. However, other phenomena occur near cutoff.

No one has yet measured the current in the time domain, but now we use the identity in Eq. (52) [4] to determine this current below the cutoff.

$$\sum_{k=1}^{\infty} \sin(kA) \equiv \frac{\sin(A)}{2[1-\cos(A)]} \text{ for } A > 0 \tag{52}$$

We use Eq. (53) for the current in the frequency domain, including all of the harmonics, but making the approximation of neglecting the effects of cutoff in Eq. (6).

$$I(t) = I_1 \sum_{k=1}^{\infty} \sin(k\omega_0 t) \tag{53}$$

Finally, we define the constant A in Eq. (52) as ωt and combine Eq. (52) with Eq. (53) to obtain Eq. (54) for the total current in the time domain. By inspection Eq. (54) is singular when $\omega_0 t$ is an even integer and zero when $\omega_0 t$ is an odd integer. Thus, the Fourier series in Eq. (53) provides singularities in determining the current as a function of time in Eq. (54) which would not be present for a finite set of harmonics.

$$I(t) = \frac{I_1 \sin(\omega_0 t)}{2[1-\cos(\omega_0 t)]} \tag{54}$$

10. Transmitting power at the harmonics with a thin-wire dipole antenna

We consider the possibility of using a thin-wire dipole antenna that is much longer than the wavelengths for a given set of selected harmonics to provide greater radiation resistance and thus increase the transmitted power. While half-wave dipoles are used in many applications, calculations suggest that the radiation resistance, and thus the radiated power for a given current has a series of maxima at frequencies where the length of the dipole is approximately 0.9, 1.9, 2.9, … wavelengths, with corresponding minima at frequencies for which the dipole lengths are between the maxima at approximately 1.4, 2.4, 3.4, … wavelengths [5]. These results are reasonable but they do not include the effects of loss caused by the resistivity of the long wire which may be appreciable.

The radiation resistance of a thin-wire dipole antenna with length L has been given by Eq. (55) [5]. Again, please note that the resistivity of the wire is not included in this equation. Here $\eta \approx 376.73\ \Omega$ is the impedance of free-space, $\gamma \approx 0.57722$ is Euler's constant, λ is the wavelength in the medium, and Ci(x) and Si(x) are the cosine and sine integrals [5]. However, there appears to be an error in this frequently used expression from Balanis so we are also studying the somewhat different equation given by Smith [6] which makes no reference to Balanis or others. The author wrote to Professor Balanis but has not yet received a response. This matter must be settled by analysis before we can proceed to study the use of dipole antennas in our application.

$$R_r = \frac{\eta}{2\pi}\left\{\begin{array}{c}\gamma + \ln\left(\frac{2\pi L}{\lambda}\right) - C_i\left(\frac{2\pi L}{\lambda}\right) + \frac{1}{2}\sin\left(\frac{2\pi L}{\lambda}\right)\left[S_i\left(\frac{4\pi L}{\lambda}\right) - 2S_i\left(\frac{2\pi L}{\lambda}\right)\right] \\ + \frac{1}{2}\cos\left(\frac{2\pi L}{\lambda}\right)\left[\gamma + \ln\left(\frac{\pi L}{\lambda}\right) + C_i\left(\frac{4\pi L}{\lambda}\right) - 2C_i\left(\frac{2\pi L}{\lambda}\right)\right]\end{array}\right\} \quad (55)$$

Consider the radiation from an antenna both with and without low-pass and high-pass filters, as well as a wide-band approach having no filters at all. The object here is to show the effect of tapering or otherwise modifying the frequency distribution of the harmonics by using filters in the nanocircuit instead of only having a sharp cutoff in the terms at the upper and lower limits for the harmonics. This is likely to require explicit summations instead of a closed-form solution for the summation.

It is interesting to compare the use of several transmitting antennas which have the same design but are scaled in size for applications at different ranges of the frequency. The usable bandwidth for each of these antennas would be proportional to its design frequency. However, this suggests that, because of the even spacing of the harmonics in the frequency comb, the number of usable harmonics, and thus the total transmitted power, would be increased by going to higher frequencies. Others have previously used thin-film long-wire antennas in which gold lines formed an ohmic contact with a semiconductor substrate having low-loss in detecting CO_2 laser radiation [7].

11. Solutions for examples

Example 1 (Fig. 4) shows the total normalized current $\Sigma I(t)/I_1$ in the 10 adjacent harmonics having indices from k_1 equal to 1 to k_2 equal to 10 calculated using Equation 8. In all eight of these examples the calculations are presented for one period of the oscillations of the mode-locked laser so that $0 \le \omega_0 t \le 2\pi$ radians.

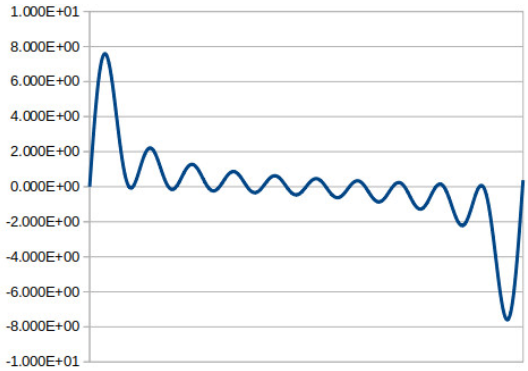

Figure 4.

Example 2 (Fig. 5) shows the total normalized current $\Sigma I(t)/I_1$ in the 50 adjacent harmonics having indices from k_1 equal to 1 to k_2 equal to 50 calculated using Equation 8.

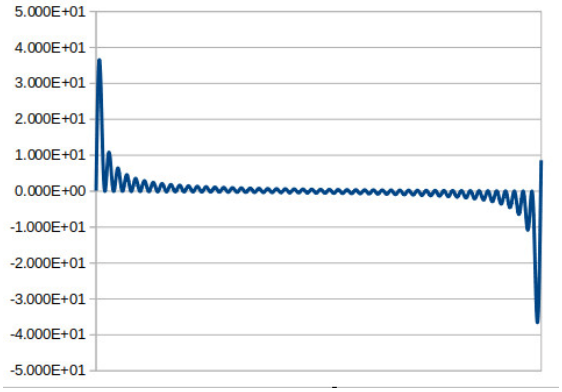

Figure 5.

Example 3 (Fig. 6) shows the total normalized current $\Sigma I(t)/I_1$ in the 100 adjacent harmonics having indices from k_1 equal to 1 to k_2 which is 100 calculated using Equation 8.

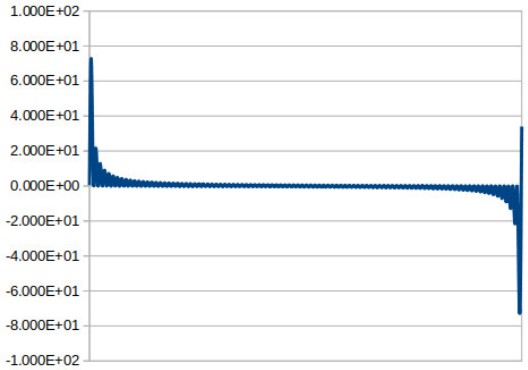

Figure 6.

Example 4 (Fig. 7) shows the total normalized current $\Sigma I(t)/I_1$ in the 500 adjacent harmonics having indices from k_1 equal to 1 to k_2 = which is 500 calculated using Equation 8.

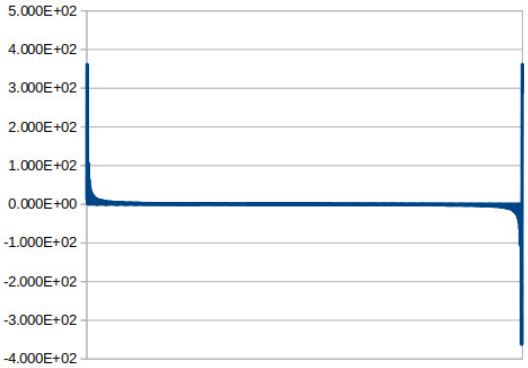

Figure 7.

Example 5 (Fig. 8) shows the total normalized current $\Sigma I(t)/I_1$ in the 20 adjacent harmonics having indices from k_1 equal to 100 to k_2 which is 120 calculated using Equation 8.

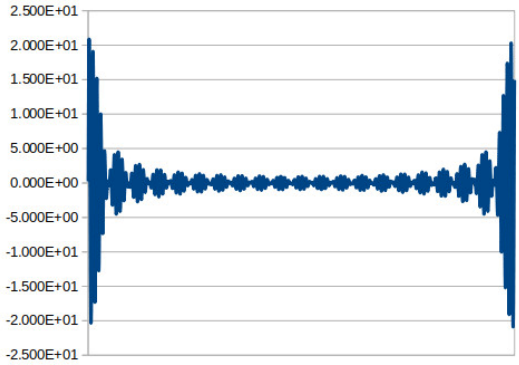

Figure 8.

Example 6 (Fig. 9) shows the total normalized current $\Sigma I(t)/I_1$ in the 20 adjacent harmonics having indices from k_1 equal to 1000 to k_2 which is 1020 calculated using Equation 8.

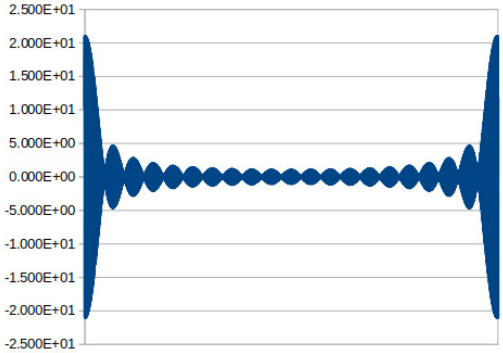

Figure 9.

Example 7 (Fig. 10) shows the total normalized current $\Sigma I(t)/I_1$ in the 200 adjacent harmonics having indices from k_1 equal to 1000 to k_2 which is 1200 calculated using Equation 8.

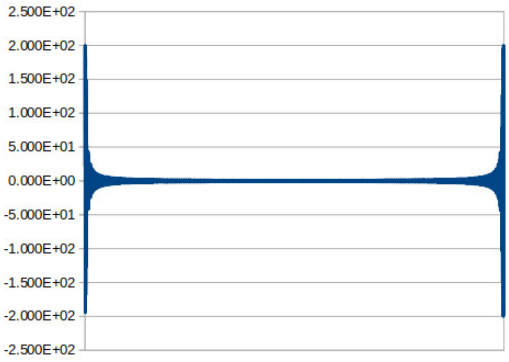

Figure 10.

Example 8 (Fig. 11) shows the total normalized current $\Sigma I(t)/I_1$ calculated using Equation 52. In this calculation it is assumed that there is an infinite number of adjacent harmonics having indices 1 to infinity, but differences in the current at each harmonic are caused by the exponential roll-off of each harmonic. Thus, in place of the sharp rise and fall at the ends of the period, there are singularities.

Figure 11.

In examples 1 through 4 we see that when a number of adjacent harmonics is chosen, that begin with k_1 equal to 1, the total current has a positive maximum near the beginning of each period and a negative maximum near the end of each period. This may be understood because the sinusoids have zero amplitude at both ends and then, because they include different frequencies, the total current has a maximum amplitude and then decays to be zero at the center of each of these 4 figures. Thus, increasing the number of harmonics increases the magnitudes of the maxima as well as the rate of decay as the center of the period is approached. In example 8, which is the extreme case for this phenomenon where effectively an infinite number of harmonics are used, there are singularities at the ends of each period.

Examples 5, 6, and 7 have a different structure because the harmonics begin with k_1 equal to 100, 1000, and 1000 instead of 1. Note that there are 20 small peaks in examples 5 and 6 which have 20 harmonics but the corresponding peaks are too small to be seen in example 7 because there are 200 harmonics.

12. Summary and Conclusions

We have derived a number of equations for studying the harmonics including the following:

Eq. 6 in section 4 is the general expression for the current in any set of the harmonics.

Eq. 8 in section 5 is a closed-form expression for the current in a set of adjacent harmonics well below the cutoff.

Eq. 19 in section 6 is a closed-form expression for the current in a set of adjacent harmonics near the cutoff.

Eq. 40 in section 7 is a closed-form expression for the current in any set of adjacent harmonics.

Eq. 54 in section 9 is a closed-form expression for the current in any large set of adjacent harmonics but neglects the exponential at the cutoff.

Section 1 introduces our previous related measurements at microwave frequencies.

Section 2 describes the proposed nanocircuit to extend the measurements to much higher frequencies. Section 10 describes the antennas that will be used to transmit these frequencies.

Section 8 describes the phenomena causing interference of the harmonics and the examples in section 11 illustrate these phenomena.

Acknowledgment

We are grateful to the Center for Integrated Nanotechnologies (CINT) program at Los Alamos National Laboratory (LANL) for making it possible for Dr. Hagmann to perform advanced studies of laser-assisted tunneling in a series of semi-annual two-week visits to LANL from 2008 to 2017. This enabled experimental verification and characterization of the microwave frequency comb that is generated when using a mode-locked laser with a scanning tunneling microscope.

References

1. M.J. Hagmann, A.J. Taylor and D.A Yarotski, "Observation of 200th harmonic with fractional linewidth of 10^{-10} in a microwave frequency comb generated in a tunneling Junction", Appl. Phys. Lett. 101 (2012) 241102.
2. M.J. Hagmann, F.S. Stenger and D.A Yarotski, "Linewidth of the harmonics in a microwave frequency comb generated by focusing a mode-locked ultrafast laser on a tunneling junction", J. Appl. Phys. 114 (2013) 223107.
3. M.J. Hagmann, D.G. Coombs and D.A. Yarotski, "Periodically pulsed laser-assisted tunneling may generate terahertz radiation", J. Vac. Sci. Technol. B 35 (2017) 03D109.
4. A.D. Whealon, A Short Table of Summable Series, Report SM-14642, (Space Technology Laboratories, Los Angeles, CA) 1953, p. 58
5. C.A. Balanis, Antenna Theory (New York, Wiley) 2nd ed., 1997, pp. 156-157, 488-498.
6. G.S. Smith, An Introduction to Classical Electromagnetic Radiation (Cambridge University Press) 1997, 600.
7. T. Shimizu, Y. Yasuoka, K. Gamo and S. Namba, "Thin-film long-wire antenna for 10.6 μm CO_2 laser radiation", Jpn. J. Appl. Phys. 31 (1992) 3359-3361.